Characterization of the Parameters of Superconducting NbN and NbTiN Films Using Parallel Plate Resonator

Fedor Khan, A. V. Khudchenko, A. M. Chekushkin, and V. P. Koshelets, *Member, IEEE*

***Abstract*—This work is dedicated to the determination of parameters of superconducting NbN and NbTiN films such as critical temperature, normal state conductivity, ratio between the gap and critical temperature and parameter incorporating the quasiparticle states inside the gap that emerge due to strong-coupling effects. The measurements were performed using a parallel plate resonator method. From the experiment, the dependence of London penetration depth on temperature was obtained. The experimental data were fitted using the expressions of Mattis-Bardeen theory extended by the consideration of strong-coupling effects. In order to design the experimental setup and visualize the results a modeling in Ansys HFSS was performed.**

***Index Terms*—Microwave measurements, niobium compounds, superconducting materials, superconducting materials measurements.**

I. Introduction

SUPERCONDUCTING materials are in a wide range of use in many different areas. Superconducting wires [1] and magnets [2] based on Nb compounds, such as Nb_3Sn and NbTi allow one to obtain the magnetic fields exceeding 10 T. Superconducting electronics devices based on Josephson tunnel junctions are being widely used in research in applied and fundamental physics: an integrated heterodyne receiver based on Superconductor-Insulator-Superconductor (SIS) junction has been used to investigate the composition of the atmosphere [3]; phonon spectra of different superconductors can be studied by measurement of current–voltage characteristics of SIS junctions [4]. Mixers based on SIS tunnel junctions have one of the lowest noise temperatures in the frequency range 100–1200 GHz, approaching the value of a quantum limit [5], and therefore are very useful in ground [6], [7] and space-based radio astronomy [8]. For new projects in this area, low-noise receivers with operating frequencies from 100 GHz to 1 THz are highly desirable [9].

However, the majority of currently used SIS receivers is produced using Nb technology and their operating frequency is therefore constrained by the gap frequency f_{gap} ($hf_{gap} = 2\Delta_0$, where Δ_0 represents a superconducting gap energy from BCS theory [10]) of Nb which is around 700 GHz. A solution for this problem may be found by fabrication and utilization of the devices based on the compounds of Nb with the higher gap frequencies, in particular, NbN and NbTiN (f_{gap} is about 1200 GHz). To produce reliable devices, it is essential to know the properties of the films and control the technological processes.

In this work we determine the following parameters of the Nb, NbN and NbTiN films: critical temperature T_c, normal state conductivity near the critical temperature σ_0, parameter of the intragap states δ, the ratio between the superconducting gap and critical temperature α and London penetration depth at zero temperature λ_0. These parameters were determined from theoretical fit of the measured dependence of London penetration depth on temperature. The description of the method and the experimental data are given in Part II. In Part III the theory to fit the experimental data is described.

II. Experiment and Results

A. Fabrication Parameters

All Nb, NbN and NbTiN films were fabricated with cluster magnetron system: Kurt J. Lesker. We used DC-mode with 500 W applied to 3-inch magnetron. High-ohmic (resistivity exceeding 5000 Ohm·cm) silicon substrate with thickness of 0.535 mm was used. The distance between substrate and magnetron was set to 6.5 mm. Substrate was cooled by running water with temperature 19 °C. Typical rate of sputtering was about 1-2 nm/s. Thicknesses of the films were chosen so that they exceed the expected value of the penetration depth. Thickness

Manuscript received September 29, 2021; revised December 17, 2021 and January 10, 2022; accepted January 25, 2022. Date of publication February 7, 2022; date of current version March 4, 2022. This work was supported by a grant from the Russian Foundation for Basic Research project No. 19-52-80023. The USU was supported by the Ministry of Science and Higher Education of the Russian Federation under Grant 075-15-2021-667. *(Corresponding author: Fedor Khan.)*

Fedor Khan is with the Kotelnikov Institute of Radioengineering and Electronics of RAS, 125009 Moscow, Russian Federation, and also with the Moscow Institute of Physics and Technology (National Research University), 141701 Moscow, Russian Federation (e-mail: khanfv@hitech.cplire.ru).

A. V. Khudchenko is with the Kotelnikov Institute of Radioengineering and Electronics of RAS, 125009 Moscow, Russian Federation, and also with the Astro Space Center of Lebedev Physical Institute of Russian Academy of Sciences, 119991 Moscow, Russian Federation (e-mail: khudchenko@asc.rssi.ru).

A. M. Chekushkin is with the Kotelnikov Institute of Radioengineering and Electronics of RAS, 125009 Moscow, Russian Federation (e-mail: chekushkin@hitech.cplire.ru).

V. P. Koshelets is with the Kotelnikov Institute of Radioengineering and Electronics of RAS, 125009 Moscow, Russian Federation (e-mail: valery@hitech.cplire.ru).

Color versions of one or more figures in this article are available at https://doi.org/10.1109/TASC.2022.3148687.

Digital Object Identifier 10.1109/TASC.2022.3148687

TABLE I
PARAMETERS OF THE SUPERCONDUCTING FILMS UNDER INVESTIGATION

Material	d (nm)	λ_0 (nm)	T_c (K)	σ_0 $\mu\Omega^{-1}m^{-1}$	δ (10^{-3})	α
Nb	250±5	90±5	9.5±0.1	13.2±0.9	1.1±1	3.6±0.09
NbN	280±5	230±20	14.8±0.3	0.62±0.04	25±3	3.9±0.08
NbN[1]	180	200	15.6	1.53	8.1	4.3
NbN[2]	41	--	14.0	1.45	70	4.1
NbTiN	320±5	210±15	14.9±0.3	1.3±0.1	15±5	3.8±0.12
NbTiN[3]	150±1	230	16.0	--	--	--
NbTiN[4]	45	--	12	0.8	--	4.0

Parameters of the Superconducting films. T_c Is the Critical temperature; σ_0 Is the Normal State DC-conductivity Near the Critical temperature; α Is a Ratio Between the Gap and Critical temperature; δ Introduces the Intragap states. λ_0 Is London Penetration Depth At Zero temperature; d Is the Thickness of the film.
[1]results for NbN Epitaxial Film From [24], [25]
[2]results for Magnetron-Sputtered NbN Film From [26]
[3]results for Magnetron Sputtered NbTiN Film From [27]
[4]results for NbTiN on Quartz From [28]

of the film was controlled by stylus profiler. Parameters of the sputtered films are listed in Table I.

B. Measurement Technique

The experiment was performed as described in [11]. A brief summary of the method is given as follows. A thin dielectric layer (15–100 μm teflon, mylar [12] or kapton [13]) is sandwiched between two superconducting films under investigation. This construction is put into a copper cavity. Two 50 Ω-microstrip lines represent the excitation system and are connected to vector network analyzer (VNA) by coaxial cables. Fig. 1 depicts the 3D models of the interior and exterior of the resonator cavity as also a photo of the cavity connected to cryogenic probe.

The resonant frequencies of rectangular resonator can be calculated using formula [11]:

$$f^2 = \frac{c^2}{\varepsilon}\left(\frac{m^2}{(2L)^2} + \frac{n^2}{(2W)^2} + \frac{p^2}{(2s)^2}\right), \qquad (1)$$

where c is the light velocity in vacuum; ε is relative permittivity of the insulator; L and W are the length and width of the superconducting film, respectively; s is the thickness of the insulating layer; m, n, p are the integers which denote index of the resonator mode.

The thickness of the insulator is more than one order of magnitude smaller than wavelength at frequencies below 20 GHz. Therefore, only the waves propagating in parallel to the surface of superconducting films can be generated and observed. Further, the numbers (m; n) from (1) will be used to denote the resonator modes. In Fig. 2 field structure of the (1; 1) resonant mode is shown.

For an insulating layer made of mylar ($\varepsilon = 3.1$) and square superconducting films with dimensions $L = W = 7$ mm, formula (1) yields a value about 17 GHz for the frequency of the resonant mode (1; 1).

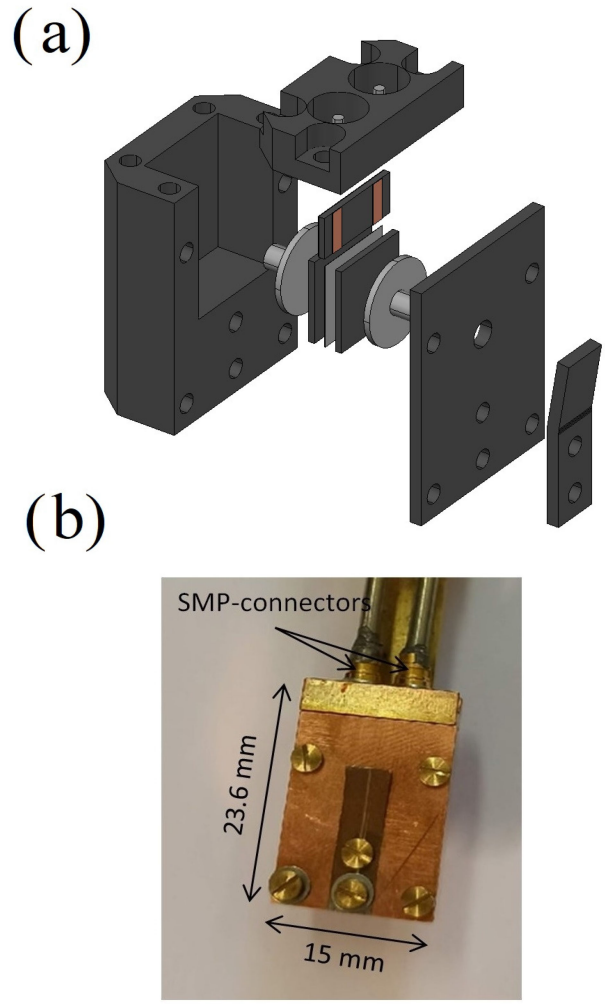

Fig. 1. (a) 3D model of the interior and exterior of the resonator cavity; (b) Photo of the resonator cavity connected to coaxial line.

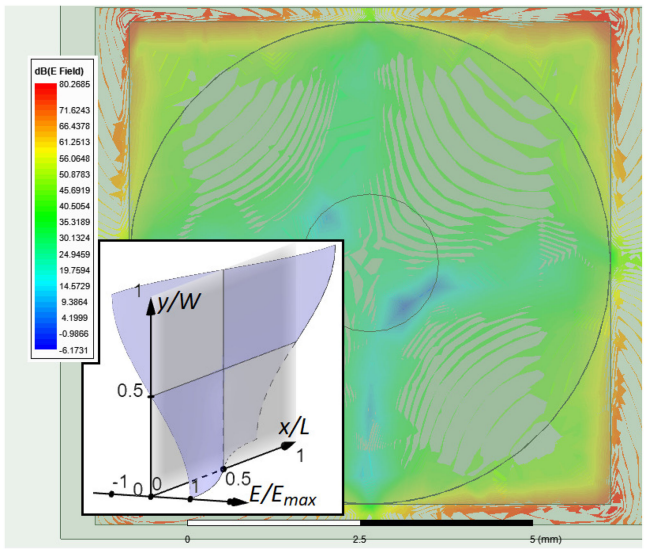

Fig. 2. Structure of electromagnetic field of the mode (1; 1) in resonator, calculated in Ansys HFSS. On the inset the draft of z-component of the electric field is shown.

C. Modeling in Ansys HFSS

With the purpose of optimizing the dimensions of the resonator cavity and visualization electromagnetic structure of the resonant modes modeling in Ansys HFSS was performed.

Effects related to superconductivity were treated by introducing special impedance boundary conditions on the surfaces of the block, which is supposed to be a superconducting film. The procedure is described in details in work [14]. Datasets for the simulation were generated using formula (7).

However, the S_{21} dependence on frequency calculated in HFSS is rather different from the experimental data, which is assumed to occur due to uncertainty in relative dielectric constant of the insulating layers, deviation of the dimensions and mechanical defects of the investigated films substrates and insulator.

D. Experimental Data

We measured S_{21} parameter directly by VNA in frequency range from 1 MHz to 20 GHz. To convince ourselves that there is minor impact on experimental data of the relative resonant frequency shift we have done several measurements with insulating films of different thickness and material. The S_{21} parameter dependence on frequency, as measured for NbTiN films separated by a 100 μm-thick mylar layer, is shown in Fig. 3(a). Among all resonant peaks only one or two correspond to superconducting parallel plate resonator. The resonant frequency of the resonance of interest can be estimated using (1). However, deviations of resonant frequencies in the experiment from calculated values are about 10% due to non-ideal open circuit boundary conditions, and calculated value of a resonant frequency may coincide with the frequency of another peak. Therefore, a more reliable method is to distinguish them from the other resonances in the cavity by higher quality factor (Q $\approx$ 300 for NbTiN films separated by 100 μm-thick mylar) and a shift in resonant frequency with the change in temperature (see Fig. 3(b)). Background oscillations on Fig. 3 are caused by standing waves in coaxial cables feeding resonator in cryogenic probe. The fit was done using the function [15]:

$$S_{21}(f) = A_1 + A_2 f + \frac{|S_{\max}| + A_3 f}{\sqrt{1 + 4\left(\frac{f - f_0}{\Delta f}\right)^2}}, \tag{2}$$

where A_1, A_2, A_3 and $|S_{max}|$ are the coefficients, f_0 is the center frequency and Δf denotes bandwidth.

The resonant frequency shift is caused by the change in phase velocity that is, in turn, related to London penetration depth by the following formula [16], [17]:

$$v = v_0 \sqrt{1 + \frac{2\Lambda}{s}}, \tag{3}$$

where v_0 is the phase velocity at zero temperature; s is the thickness of the insulating layer; Λ is the effective London penetration depth with correction made for a finite thickness

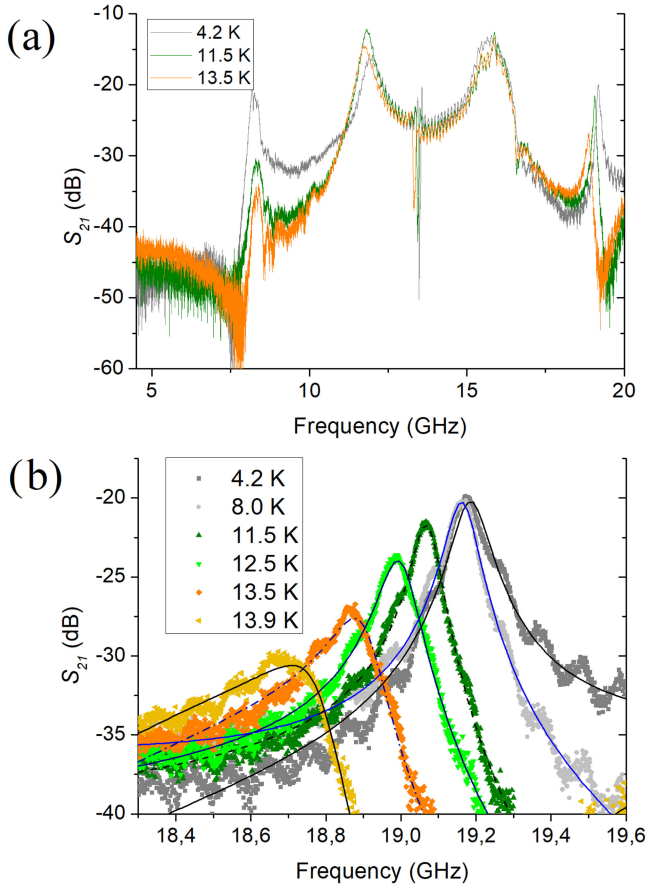

Fig. 3. (a) S_{21} parameter as a function of frequency measured at different temperatures for NbTiN films separated by 100 μm-thick mylar. Frequencies below 5 GHz and some of the curves at intermediate temperatures are omitted in order to improve visibility. (b) Enlarged image of a resonant peak with frequency about 19 GHz, corresponding to (1; 1)-resonant mode. Solid lines represent fit for the experimental data using formula (2).

of superconductive film in case of small surface resistance [18]:

$$\Lambda = \lambda \coth\left(\frac{d}{\lambda}\right) \tag{4}$$

Here, λ is London penetration depth; d is the thickness of the superconducting film.

Equation (3) can be also rewritten in terms of resonant frequencies using (1):

$$\frac{F(T) - F_0}{F_0} = \frac{\sqrt{1 + \frac{2\Lambda_0}{s}}}{\sqrt{1 + \frac{2\Lambda(T)}{s}}} - 1, \tag{5}$$

where Λ_0 and F_0 are effective London penetration depth and resonant frequency at temperature $T = 4.2$ K, respectively.

Fig. 4 shows the dependence of the relative shift in resonant frequency on temperature. The experimental data (marked with points) are extracted from the measurements similar to that of Fig. 3 for corresponding superconducting films and insulating layers. The theoretical fit (solid lines) is done using equation (5) with $\Lambda(T)$ introduced in the following section. Formulae (3) and (4) enable us to calculate the London penetration depth of the

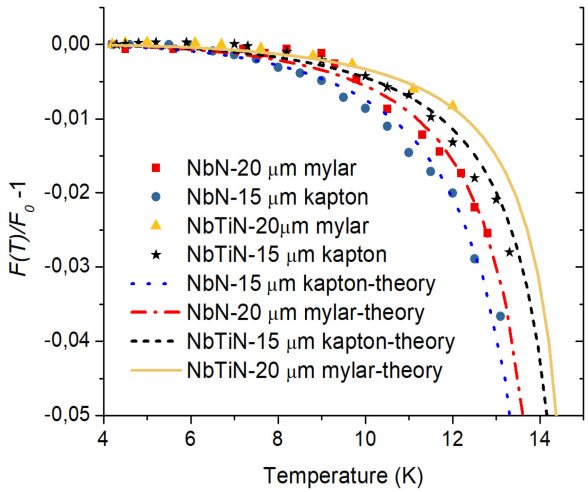

Fig. 4. Relative shift in resonant frequency depending on temperature for NbN and NbTiN films measured using 15 μm kapton and 20 μm-thick mylar layers. Measurements for Nb are omitted in order to improve visibility of the plot. F_0 is the resonant frequency at 4.2 K.

films under investigation. Transition from effective penetration depth to that of a bulk film was done by fixed-point iteration method applied to formula (4). The corresponding result is shown in Fig. 5.

III. Expression for London Penetration Depth

London penetration depth is related to the surface impedance by the following formula [19]:

$$\Lambda = \frac{X}{\omega \mu_0}, \tag{6}$$

where X is the imaginary part of the surface impedance; ω is angular frequency; μ_0 is magnetic permeability of vacuum.

The surface impedance of superconducting film in dirty limit (mean free pass length is much smaller than London penetration depth and wavelength, which is valid for magnetron-sputtered films) can be calculated numerically using the expressions for conductivity σ from Mattis and Bardeen theory [20] inserted into the formula below [21]:

$$Z = \sqrt{\frac{i\omega\mu_0}{\sigma}} \coth\left(\sqrt{i\omega\mu_0\sigma} d\right), \tag{7}$$

However, for materials such as Nb, NbN and NbTiN strong-coupling effects lead to appearance of the intragap states for quasiparticle excitations [22], [23]. This effect can be taken into account by adding a small imaginary part to the superconducting gap [23], [24]: $\Delta = \Delta_0 (1+i\delta)$.

Moreover, in the relation $2\Delta = \alpha k_B T_c$, the parameter α is not equal to 3.52 as in common BCS superconductors. Here, k_B is the Boltzmann constant; T_c is the critical temperature.

By inserting the imaginary part of the surface impedance from (7) into (6) and then using this result in formula (5), we obtain a function of variables (σ_0, α, δ, T_c) to fit the experimental data on Fig. 4. Fitting procedure and an estimation of the errors of the parameters were carried out using a least-squares method. The parameters obtained in the result of fitting and

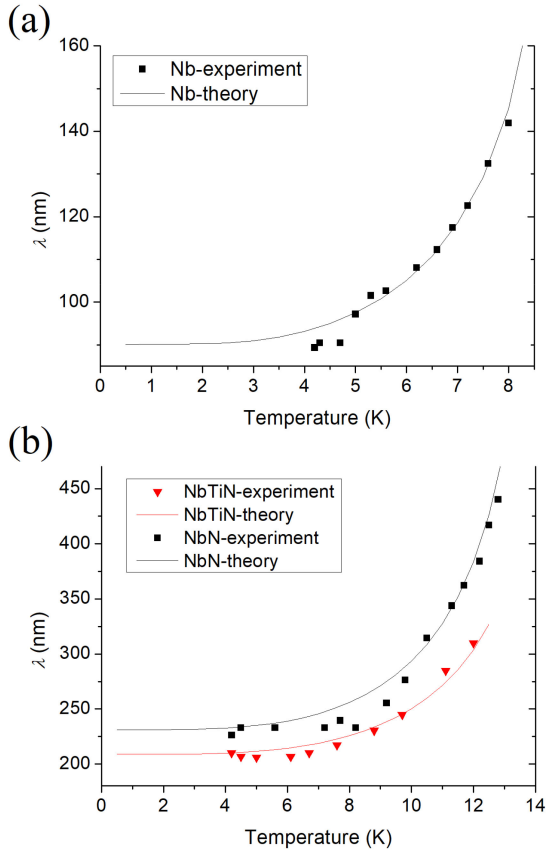

Fig. 5. London penetration depth dependence on temperature for Nb (a) and NbN and NbTiN films (b). Experimental data are shown with markers. Solid lines represent the result obtained by fixed-point iteration method using formula (4) and substituting Λ from (6) and (7) into it with the parameters obtained from the best-fit.

DC-measurements are listed in Table I. The main source of the uncertainty in determination of the parameters appears due to temperature measurements due to inhomogeneity of the temperature across the sample. We also neglected the dependence of permittivity of the insulating layers on temperature that, in turn, may lead to additional error.

IV. Conclusion

To sum up, we measured the parameters of superconducting Nb, NbN and NbTiN films using a resonator, and derived theoretical expressions to fit the experimental data considering strong-coupling effects. The obtained data are in good agreement with the values provided in the literature by other authors. See Table I and references [25], [26] for NbN and [27], [28] for NbTiN measurements. The data obtained can be helpful in fabrication of new superconductive devices.

Acknowledgment>

The equipment of USU #352529"Cryointegral" was used to carry out the research.

REFERENCES

[1] A. Godeke, "A review of the properties of Nb_3Sn and their variation with A15 composition, morphology and strain state," *Supercond. Sci. Technol.*, vol. 19, no. 8, pp. R68–R80, 2006, doi: 10.1088/09532048/19/8/R02.

[2] X. Xu, "A review and prospects for Nb_3Sn superconductor development," *Supercond. Sci. Technol.*, vol. 30, no. 9, 2017, Art. no. 093001, doi: 10.1088/1361-6668/aa7976.

[3] A. de Lange *et al.*, "HCl and ClO in activated Arctic air; first retrieved vertical profiles from TELIS submillimetre limb spectra," *Atmos. Meas. Tech.*, vol. 5, no. 2, pp. 487–500, 2012, doi: 10.5194/amt-5-487-2012.

[4] W. E. Bron, "Spectroscopy of high-frequency phonons," *Rep. Prog. Phys.*, vol. 43, no. 3, pp. 301–352, 1980, doi: 10.1088/0034-4885/43/3/002.

[5] T. Kojima *et al.*, "Three quanta sensitivity superconductor–insulator–superconductor mixer for the 0.78–0.95 THz band," *Appl. Phys. Express*, vol. 2, no. 10, 2009, Art. no. 102201, doi: 10.1143/APEX.2.102201.

[6] "ALMA observatory." Accessed: Feb. 11, 2022. [Online]. Available: https://www.almaobservatory.org/

[7] "APEX telescope." [Online]. Available: https://www.apex-telescope.org/

[8] "Millimetron space observatory." [Online]. Available: https://millimetron.ru/

[9] S. I. Asayama *et al.*, "ALMA band 10 (787-950 GHz) first astronomical fringes," in *Ground-Based and Airborne Telescopesin V*, Montréal, 2014, pp. 1578–1587.

[10] J. Bardeen, L. N. Cooper, and J. R. Schrieffer, "Theory of superconductivity," *Phys. Rev.*, vol. 108, no. 5, pp. 1175–1204, 1957, doi: 10.1103/PhysRev.108.1175.

[11] R. C. Taber, "A parallel plate resonator technique for microwave loss measurements on superconductors," *Rev. Sci. Instrum.*, vol. 61, no. 8, pp. 2200–2206, 1990, doi: 10.1063/1.1141389.

[12] D. C. Dube and R. Natarajan, "Measurement of the permittivity of films at microwave frequencies," *J. Phys. E: Scientific Instrum.*, vol. 7, no. 4, pp. 256–257, 1974, doi: 10.1088/0022-3735/7/4/012.

[13] "DuPont datasheet." Accessed: Feb. 11, 2022. [Online]. Available: https://www.pp.dupont.com/products/kapton-hn.html

[14] V. Belitsky *et al.*, "Superconducting microstrip line model studies at millimetre and sub-millimetre waves," *Int. J. Infrared Millimeter Waves*, vol. 27, no. 6, pp. 809–834, 2007, doi: 10.1007/s10762-006-9116-5.

[15] P. J. Petersan and S. M. Anlage, "Measurement of resonant frequency and quality factor of microwave resonators: Comparison of methods," *J. Appl. Phys.*, vol. 84, no. 6, pp. 3392–3402, 1998, doi: 10.1063/1.368498.

[16] J. C. Swihart, "Field solution for a thin-film superconducting strip transmission line," *J. Appl. Phys.*, vol. 32, no. 3, pp. 461–469, 1961, doi: 10.1063/1.1736025.

[17] R. L. Kautz, "Picosecond pulses on superconducting striplines," *J. Appl. Phys.*, vol. 49, no. 1, pp. 308–314, 1978, doi: 10.1063/1.324387.

[18] N. Klein *et al.*, "The effective microwave surface impedance of high T_c thin films," *J. Appl. Phys.*, vol. 67, no. 11, pp. 6940–6945, 1990, doi: 10.1063/1.345037.

[19] M. A. Biondi and M. P. Garfunkel, "Millimeter wave absorption in superconducting aluminum. II. Calculation of the skin depth," *Phys. Rev.*, vol. 116, no. 4, pp. 862–867, 1959, doi: 10.1103/PhysRev.116.862.

[20] D. C. Mattis and J. Bardeen, "Theory of the anomalous skin effect in normal and superconducting metals," *Phys. Rev.*, vol. 111, no. 2, pp. 412–417, 1958, doi: 10.1103/PhysRev.111.412.

[21] G. R. Henry, "Anomalous skin effect in thin films," *J. Appl. Phys.*, vol. 43, no. 7, pp. 2996–3001, 1972, doi: 10.1063/1.1661647.

[22] S. B. Kaplan *et al.*, "Quasiparticle and phonon lifetimes in superconductors," *Phys. Rev. B*, vol. 14, no. 11, pp. 4854–4873, 1976, doi: 10.1103/PhysRevB.14.4854.

[23] B. Mitrović and L. A. Rozema, "On the correct formula for the lifetime broadened superconducting density of states," *J. Phys.: Condens. Matter*, vol. 20, no. 1, 2008, Art. no. 015215, doi: 10.1088/0953-8984/20/01/015215.

[24] T. Noguchi *et al.*, "RF conductivity and surface impedance of a superconductor taking into account the complex superconducting gap energy," *Phys. Procedia*, vol. 36, pp. 318–323, 2012, doi: 10.1016/j.phpro.2012.06.166.

[25] A. Kawakami *et al.*, "Estimation of surface resistance for epitaxial NbN films in the frequency range of 0.1-1.1 THz," *IEEE Trans. Appl. Supercond.*, vol. 13, no. 2, pp. 1147–1150, Jun. 2003, doi: 10.1109/TASC.2003.814177.

[26] Y. Uzawa *et al.*, "Optical and tunneling studies of energy gap in superconducting niobium nitride films," *J. Low Temp. Phys.*, vol. 199, pp. 143–148, 2020, doi: 10.1007/s10909-019-02324-1.

[27] L. Yu *et al.*, "Fabrication of niobium titanium nitride thin films with high superconducting transition temperatures and short penetration lengths," *IEEE Trans. Appl. Supercond.*, vol. 15, no. 1, pp. 44–48, Mar. 2005, doi: 10.1109/TASC.2005.844126.

[28] Y. Uzawa *et al.*, "Tuning circuit material for mass-produced terahertz SIS receivers," *IEEE Trans. Appl. Supercond.*, vol. 25, no. 3, Jun. 2015, Art. no. 2401005, doi: 10.1109/TASC.2014.2386211.